How to treat the coupling issue of the Saint-Venant-Exner system of equations

Philippe Ung[1,4]

joint work with
Emmanuel Audusse[1,2], Christophe Chalons[3]

[1]Team ANGE – CEREMA, Inria Rocquencourt, LJLL
[2]LAGA – Université Paris XIII
[3]LMV – Université de Versailles Saint-Quentin-en-Yvelines
[4]MAPMO – Université d'Orléans

Egrin
June 1st, 2015

Outline

Context & Motivations

Motivations
Framework

Sediments transport is responsible of modification of river beds.

2 processes of sediments transport:

- by suspension: particles can be found on the whole vertical water depth and rarely be in contact with the bed,
- by bedload: particles are moving near the bed by saltation and rolling.

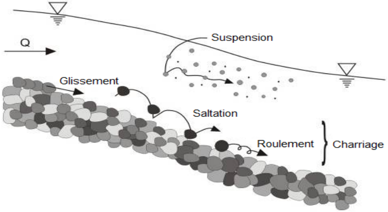

Figure: Processes of sediment transport.

Thereafter, we only focuse on the **bedload transport**.

Saint-Venant–Exner equations
The model

In the literature, most of industrial codes use the **Saint-Venant–Exner model**.

$$\begin{cases} \partial_t H + \partial_x (Q) = 0, & \text{(1a)} \\ \partial_t Q + \partial_x \left(\dfrac{Q^2}{H} + \dfrac{gH^2}{2} \right) = -gH\partial_x B - \dfrac{\tau}{\rho}. & \text{(1b)} \\ \partial_t B + \partial_x Q_s = 0, & \text{(1c)} \end{cases}$$

Coupled model between:

- the Saint-Venant equations (aka shallow-water equations): (1a)–(1b)

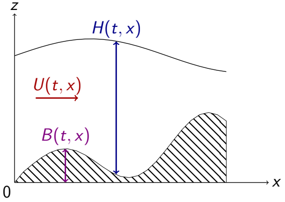

$H(t,x)$: water height,
$Q(t,x) = HU$: discharge,
$B(t,x)$: bottom topography,
with $x \in \Omega \subseteq \mathbb{R}$, $t \geqslant 0$.

Saint-Venant–Exner equations
The model

τ is defined by the **Manning formula**,

$$\tau = \rho g H \frac{Q|Q|}{H^2 \, K_s^2 \, R_h^{4/3}}, \tag{2}$$

where, in the particular case of a rectangular channel with width l, the hydraulic radius R_h reads

$$R_h = \frac{lH}{l + 2H}.$$

Saint-Venant–Exner equations
The model

- the Exner equation (1c)

where $Q_s(t,x)$ is the solid transport flux defined by

$$Q_s = \sqrt{\frac{g(\rho_s - \rho)d^3}{\rho}} Q_s^\star\left(\tau^\star; \tau_c^\star\right) \frac{\tau^\star}{|\tau^\star|} \tag{3}$$

and the **Meyer-Peter-Müller formula**,

$$Q_s^\star = A\left(|\tau^\star| - \tau_c^\star\right)_+^{3/2} \tag{4}$$

$$\text{with} \begin{cases} A & \text{a constant,} \\ \rho_s,\ \rho & \text{resp. the mass densities of the solid and fluid phases,} \\ g & \text{the gravitational acceleration,} \\ \tau^\star & \text{the shear stress (aka Shields parameter),} \\ \tau_c^\star & \text{the critical value for the initiation of motion,} \\ d & \text{the grain diameter.} \end{cases}$$

Saint-Venant–Exner equations
The model

A more practical expression of the solid discharge

- Grass formula,

$$Q_s = A_g U |U|^{m-1} \tag{5}$$

where A_g is an empirically determined constant and $0 < m < 4$.

Saint-Venant–Exner equations
The model

The Saint-Venant–Exner equations can be rewritten in a vectorial form,

$$\partial_t \tilde{W} + \partial_x F(\tilde{W}) = S(\tilde{W}), \tag{6}$$

where

$$\tilde{W} = \begin{pmatrix} H \\ HU \\ B \end{pmatrix}, \quad F(\tilde{W}) = \begin{pmatrix} HU \\ HU^2 + \dfrac{gH^2}{2} \\ Q_s \end{pmatrix},$$

$$S(\tilde{W}) = \begin{pmatrix} 0 \\ -gH\partial_x B \\ 0 \end{pmatrix}.$$

Quasilinear form:

$$\partial_t \tilde{W} + A(\tilde{W})\partial_x \tilde{W} = S(\tilde{W}),$$

where A is the jacobian matrix of F.

Motivations

Numerical aspect

Two strategies to approximate the solution of the system:

splitting and non-splitting methods.

Motivations

Numerical aspect

Two strategies to approximate the solution of the system:

splitting and non-splitting methods.

The problem of choice between these two methods remains when considering “fast flow” (Hudson et al, 2003 & 2005):

Motivations
Numerical aspect

Two strategies to approximate the solution of the system:

splitting and non-splitting methods.

The problem of choice between these two methods remains when considering “fast flow” (Hudson et al, 2003 & 2005):

- the splitting method injects numerical instabilities,

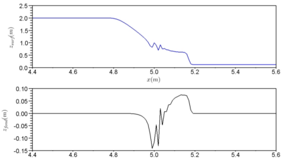

Figure: Free surface (top) and Bottom topography (bottom)

Motivations

Numerical aspect

- the non-splitting method allows to correct these instabilities,
  - Roe-type solver (Hudson et al. 2003 & 2005, Murillo and Garcia-Navarro 2010),
  - Intermediate Field Capturing Riemann solver (Pares 2006, Pares et al. 2011),
  - Relaxation scheme (Delis et al. 2008, ABCDGJSGS 2011),
  - Non Homogeneous Riemann solver (Benkhaldoun et al. 2009),
  - Godunov-type method based on a three-waves Approximate Riemann Solver (ARS).

Numerical scheme

Numerical approximation
Properties & Main definitions

- **Positivity** of water height,

$$H \geqslant 0\,,$$

Numerical approximation
Properties & Main definitions

- **Positivity** of water height,

$$H \geqslant 0\,,$$

- **Well-balanced** property or ability to preserve steady states of the lake at rest,

$$U = 0\,, \qquad H + B = Cte\,.$$

Numerical approximation
Properties & Main definitions

- **Positivity** of water height,

$$H \geqslant 0\,,$$

- **Well-balanced** property or ability to preserve steady states of the lake at rest,

$$U = 0\,, \qquad H + B = Cte\,.$$

- **Froude number**,

$$F_r = \frac{|U|}{\sqrt{gH}}. \tag{7}$$

$F_r < 1$ Fluvial regime,
$F_r = 1$ Transcritical regime,
$F_r > 1$ Torrential regime.

Numerical scheme

Objective

Main objective

Developping a non-splitted method to solve the Saint-Venant–Exner system.

Strategy

Propose a Godunov-type method to solve the Saint-Venant–Exner equations based on the design of a **three-wave Approximate Riemann Solver** which is able to degenerate to an ARS satisfying all these properties together when the solid flux is null, sufficiently **easy to compute**.

Numerical scheme
Discretization

Space discretization Ω, $\forall i \in \mathbb{Z}$

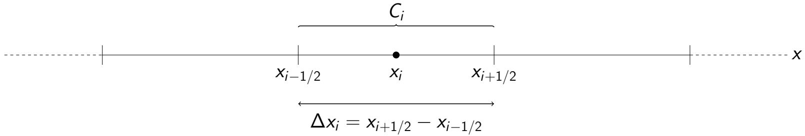

N_x: Number of cells.

Time discretization $t \geqslant 0$, $\forall n \in \mathbb{N}$

$$t^{n+1} = t^n + \Delta t^n , \qquad \Delta t > 0.$$

In the following, we denote

$$\Delta x_i = \Delta x , \qquad \Delta t^n = \Delta t .$$

Numerical scheme
Main ideas

Notations: $\forall X \in \{H, HU, B\}$,

$$X_L \approx \frac{1}{\Delta x}\int_{-\Delta x}^{0} X(x)dx\,;\, X_R \approx \frac{1}{\Delta x}\int_{0}^{\Delta x} X(x)dx\,;\, X_i \approx \frac{1}{\Delta x}\int_{C_i} X(x)dx\,.$$

Numerical scheme
Main ideas

Notations: $\forall X \in \{H, HU, B\}$,

$$X_L \approx \frac{1}{\Delta x}\int_{-\Delta x}^{0} X(x)dx\,;X_R \approx \frac{1}{\Delta x}\int_{0}^{\Delta x} X(x)dx\,;X_i \approx \frac{1}{\Delta x}\int_{C_i} X(x)dx\,.$$

At t^n, $\tilde{W}_i^n = (W_i^n, B_i^n) = (H_i^n, H_i^n U_i^n, B_i^n)^T$ a given piecewise constant approximate solution,

Numerical scheme

Main ideas

Notations: $\forall X \in \{H, HU, B\}$,

$$X_L \approx \frac{1}{\Delta x}\int_{-\Delta x}^{0} X(x)dx\,; X_R \approx \frac{1}{\Delta x}\int_{0}^{\Delta x} X(x)dx\,; X_i \approx \frac{1}{\Delta x}\int_{C_i} X(x)dx\,.$$

At t^n, $\tilde{W}_i^n = (W_i^n,\, B_i^n) = (H_i^n,\, H_i^n U_i^n,\, B_i^n)^T$ a given piecewise constant approximate solution,

- Building an approximate solution of the Riemann problem at each interface $x_{i+1/2}$,

Numerical scheme

Main ideas

Notations: $\forall X \in \{H, HU, B\}$,

$$X_L \approx \frac{1}{\Delta x}\int_{-\Delta x}^{0} X(x)dx\,; X_R \approx \frac{1}{\Delta x}\int_{0}^{\Delta x} X(x)dx\,; X_i \approx \frac{1}{\Delta x}\int_{C_i} X(x)dx\,.$$

At t^n, $\tilde{W}_i^n = (W_i^n,\, B_i^n) = (H_i^n,\, H_i^n U_i^n,\, B_i^n)^T$ a given piecewise constant approximate solution,

- Building an approximate solution of the Riemann problem at each interface $x_{i+1/2}$,
- Definition of $\tilde{W}_i^{n+1} = (W_i^{n+1},\, B_i^{n+1})$ by calculating the average value of the juxtaposition of these solutions in each cell C_i at time t^{n+1}.

Numerical scheme

Riemann problem

A simple Approximate Riemann Solver composed by three waves propagating with velocities λ_L, $\lambda_0 = 0$ and λ_R such as

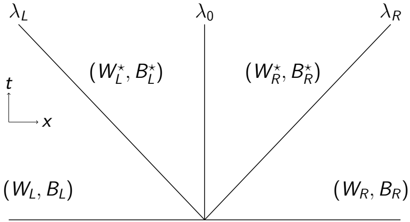

Figure: Local Riemann problem

$$\lambda_L \leqslant 0 \leqslant \lambda_R.$$

gives an approximate Riemann solution associated with initial data

$$(W(0,x),\ B(0,x)) = \begin{cases} (W_L,\ B_L) & ,\ x < 0, \\ (W_R,\ B_R) & ,\ x > 0. \end{cases}$$

CFL condition: $\Delta t < \dfrac{\Delta x}{2\max(|\lambda_L|, \lambda_R)}$.

Numerical scheme
Consistency

Consistency

$$F(\tilde{W}_R) - F(\tilde{W}_L) - S\left(\tilde{W}_L,\ \tilde{W}_R\right) = \lambda_L(\tilde{W}_L^* - \tilde{W}_L) + \lambda_R(\tilde{W}_R - \tilde{W}_R^*),$$

with

$$\lim_{\substack{\tilde{W}_L,\, \tilde{W}_R \to \tilde{W} \\ \Delta x \to 0}} \frac{1}{\Delta x} S\left(\tilde{W}_L,\ \tilde{W}_R\right) = (0,\ -gH\partial_x B,\ 0)^T .$$

Relations of consistency in the integral form:

$$\begin{cases} H_R U_R - H_L U_L = \lambda_L \left(H_L^\star - H_L\right) + \lambda_R \left(H_R - H_R^\star\right), & (8) \\ \left(H_R U_R^2 + \dfrac{g H_R^2}{2}\right) - \left(H_L U_L^2 + \dfrac{g H_L^2}{2}\right) + g\Delta x\{H\partial_x B\} & \\ \qquad = \lambda_L \left(H_L^\star U_L^\star - H_L U_L\right) + \lambda_R \left(H_R U_R - H_R^\star U_R^\star\right), & (9) \\ Q_{sR} - Q_{sL} = \lambda_L \left(B_L^\star - B_L\right) + \lambda_R \left(B_R - B_R^\star\right). & (10) \end{cases}$$

Numerical approximation of the Saint-Venant–Exner equations

Definition of the intermediate states

Relations of continuity across the stationary wave:

$$\begin{cases} H_L^\star + B_L^\star = H_R^\star + B_R^\star, & (11) \\ H_L^\star U_L^\star = H_R^\star U_R^\star. & (12) \end{cases}$$

We add a minimization problem

$$\min F(B_L^\star, B_R^\star) = \left(||B_L - B_L^\star||^2 + ||B_R - B_R^\star||^2 \right)$$
$$u.c.\ \lambda_L \left(B_L^\star - B_L \right) + \lambda_R \left(B_R - B_R^\star \right) - \left(Q_{sR} - Q_{sL} \right) = 0$$

Numerical approximation of the Saint-Venant–Exner equations

Definition of the intermediate states

Relations of continuity across the stationary wave:

$$\begin{cases} H_L^\star + B_L^\star = H_R^\star + B_R^\star, & (11) \\ H_L^\star U_L^\star = H_R^\star U_R^\star. & (12) \end{cases}$$

We add a minimization problem

$$\min F(B_L^\star, B_R^\star) = \left(||B_L - B_L^\star||^2 + ||B_R - B_R^\star||^2\right)$$
$$u.c.\ \lambda_L \left(B_L^\star - B_L\right) + \lambda_R \left(B_R - B_R^\star\right) - \left(Q_{sR} - Q_{sL}\right) = 0$$

$$B_L^\star = B_L + \frac{\lambda_L}{\lambda_L^2 + \lambda_R^2} \Delta Q_s, \qquad (13)$$

$$B_R^\star = B_R - \frac{\lambda_R}{\lambda_L^2 + \lambda_R^2} \Delta Q_s, \qquad (14)$$

Numerical scheme

Definition of the intermediate states: Well-balanced property

$$Q^\star := H_L^\star U_L^\star = H_R^\star U_R^\star,$$
$$Q^\star = Q_{HLL} - \frac{g}{\lambda_R - \lambda_L} \Delta x \{H \partial_x B\}, \tag{15}$$

with

$$Q_{HLL} = \frac{\lambda_R H_R U_R - \lambda_L H_L U_L}{\lambda_R - \lambda_L} - \frac{\left(H_R U_R^2 + \frac{g H_R^2}{2}\right) - \left(H_L U_L^2 + \frac{g H_L^2}{2}\right)}{\lambda_R - \lambda_L},$$

Numerical scheme

Definition of the intermediate states: Well-balanced property

$$Q^\star := H_L^\star U_L^\star = H_R^\star U_R^\star,$$

$$Q^\star = Q_{HLL} - \frac{g}{\lambda_R - \lambda_L} \Delta x \{H \partial_x B\}, \tag{15}$$

with

$$Q_{HLL} = \frac{\lambda_R H_R U_R - \lambda_L H_L U_L}{\lambda_R - \lambda_L} - \frac{\left(H_R U_R^2 + \frac{g H_R^2}{2}\right) - \left(H_L U_L^2 + \frac{g H_L^2}{2}\right)}{\lambda_R - \lambda_L},$$

Well-balanced property ensures by

$$\{H \partial_x B\} = \begin{cases} \frac{H_L + H_R}{2\Delta x} \, min \left(H_L, \Delta B\right) & \text{if } \Delta B^\star \geqslant 0, \\ \frac{H_L + H_R}{2\Delta x} \, max \left(-H_R, \Delta B\right) & \text{if } \Delta B^\star < 0. \end{cases}$$

Numerical approximation of the Saint-Venant–Exner equations

Definition of the intermediate states: Positivity of the water height

$$H_L^\star = H_{HLL} + \frac{\lambda_R}{\lambda_R - \lambda_L}\Delta B^\star, \tag{17}$$

$$H_R^\star = H_{HLL} + \frac{\lambda_L}{\lambda_R - \lambda_L}\Delta B^\star, \tag{18}$$

with

$$H_{HLL} = \frac{\lambda_R H_R - \lambda_L H_L}{\lambda_R - \lambda_L} - \frac{1}{\lambda_R - \lambda_L}\left(H_R U_R - H_L U_L\right). \tag{19}$$

Numerical approximation of the Saint-Venant–Exner equations

Definition of the intermediate states: Positivity of the water height

$$H_L^\star = H_{HLL} + \frac{\lambda_R}{\lambda_R - \lambda_L}\Delta B^\star, \tag{17}$$

$$H_R^\star = H_{HLL} + \frac{\lambda_L}{\lambda_R - \lambda_L}\Delta B^\star, \tag{18}$$

with

$$H_{HLL} = \frac{\lambda_R H_R - \lambda_L H_L}{\lambda_R - \lambda_L} - \frac{1}{\lambda_R - \lambda_L}\left(H_R U_R - H_L U_L\right). \tag{19}$$

If $\Delta B^\star \geqslant 0$,	If $\Delta B^\star < 0$,
$\lambda_R \tilde{H}_R^\star = max\left(\lambda_R H_R^\star, 0\right),$ $\lambda_L \tilde{H}_L^\star = \lambda_L H_L^\star - \lambda_R\left(H_R^\star - \tilde{H}_R^\star\right),$	$\lambda_L \tilde{H}_L^\star = max\left(\lambda_L H_L^\star, 0\right)$ $\lambda_R \tilde{H}_R^\star = \lambda_R H_R^* - \lambda_L\left(H_L^\star - \tilde{H}_L^\star\right)$

Numerical approximation of the Saint-Venant–Exner equations

Definition of the wave velocities

The main issue comes from the **choice of** λ_L **and** λ_R.

Numerical approximation of the Saint-Venant–Exner equations

Definition of the wave velocities

The main issue comes from the **choice of λ_L and λ_R**.
Recall

$$A(\tilde{W}) = \begin{bmatrix} 0 & 1 & 0 \\ gH - U^2 & 2U & gH \\ \tilde{\alpha} & \tilde{\beta} & 0 \end{bmatrix}$$

where $\tilde{\alpha} = \dfrac{\partial Q_s}{\partial H}$ and $\tilde{\beta} = \dfrac{\partial Q_s}{\partial Q}$.

Numerical approximation of the Saint-Venant–Exner equations

Definition of the wave velocities

The main issue comes from the **choice of λ_L and λ_R.**
Recall

$$A(\tilde{W}) = \begin{bmatrix} 0 & 1 & 0 \\ gH - U^2 & 2U & gH \\ \tilde{\alpha} & \tilde{\beta} & 0 \end{bmatrix}$$

where $\tilde{\alpha} = \dfrac{\partial Q_s}{\partial H}$ and $\tilde{\beta} = \dfrac{\partial Q_s}{\partial Q}$.

Characteristic polynomial of A:

$$p_A(\lambda) = \lambda^3 - 2U\lambda^2 - (gH(1+\tilde{\beta}) - U^2)\lambda - gH\tilde{\alpha} = 0. \qquad (20)$$

Numerical approximation of the Saint-Venant–Exner equations

Definition of the wave velocities: Nickalls' bounds (2011)

Derivative quadratic equation of p_A:

$$3\lambda^2 - 4U\lambda - (gH(1+\tilde{\beta}) - U^2) = 0. \tag{21}$$

Numerical approximation of the Saint-Venant–Exner equations

Definition of the wave velocities: Nickalls' bounds (2011)

Derivative quadratic equation of p_A:

$$3\lambda^2 - 4U\lambda - (gH(1+\tilde{\beta}) - U^2) = 0. \tag{21}$$

The solutions are

$$\lambda_\pm = x_0 \pm \Omega, \tag{22}$$

such as $x_0 = \dfrac{2U}{3}$ and $\Omega = \dfrac{1}{3}\sqrt{U^2 + 3gH(1+\tilde{\beta})}$.

Numerical approximation of the Saint-Venant–Exner equations

Definition of the wave velocities: Nickalls' bounds (2011)

Derivative quadratic equation of p_A:

$$3\lambda^2 - 4U\lambda - (gH(1+\tilde{\beta}) - U^2) = 0. \tag{21}$$

The solutions are

$$\lambda_{\pm} = x_0 \pm \Omega, \tag{22}$$

such as $x_0 = \dfrac{2U}{3}$ and $\Omega = \dfrac{1}{3}\sqrt{U^2 + 3gH(1+\tilde{\beta})}$.

The wave velocities are defined by

$$\lambda_L = x_0 - 2\,\Omega, \tag{23}$$

$$\lambda_R = x_0 + 2\,\Omega. \tag{24}$$

Numerical scheme
Summary

Associated Godunov-type scheme

$$\begin{cases} \tilde{W}_i^{n+1} = \tilde{W}_i^n - \dfrac{\Delta t^n}{\Delta x}(F^-_{i+1/2} - F^+_{i-1/2})\,, \\ \tilde{W}_i^0 = \dfrac{1}{\Delta x}\left(\displaystyle\int_{C_i} H_0(x)dx,\ \int_{C_i}(H_0 U_0)(x)dx,\ \int_{C_i} B_0(x)dx\right)^T, \end{cases}$$

where F^- and F^+ are given by

$$\begin{cases} F^-(\tilde{W}_L,\ \tilde{W}_R) = F(\tilde{W}_L) + \lambda_L\left(\tilde{W}_L^\star - \tilde{W}_L\right)\,, \\ F^+(\tilde{W}_L,\ \tilde{W}_R) = F(\tilde{W}_R) + \lambda_R\left(\tilde{W}_R^\star - \tilde{W}_R\right)\,, \end{cases}$$

and the wave velocities are defined by

$$\lambda_L = x_0 - 2\,\Omega,$$
$$\lambda_R = x_0 + 2\,\Omega,$$

with $x_0 = \dfrac{2U}{3}$ and $\Omega = \dfrac{1}{3}\sqrt{U^2 + 3gH(1+\tilde{\beta})}$ and $\tilde{\beta} = \dfrac{\partial Q_s}{\partial Q}$.

Test cases

Numerical results

Evolution of a bump in a fluvial regime

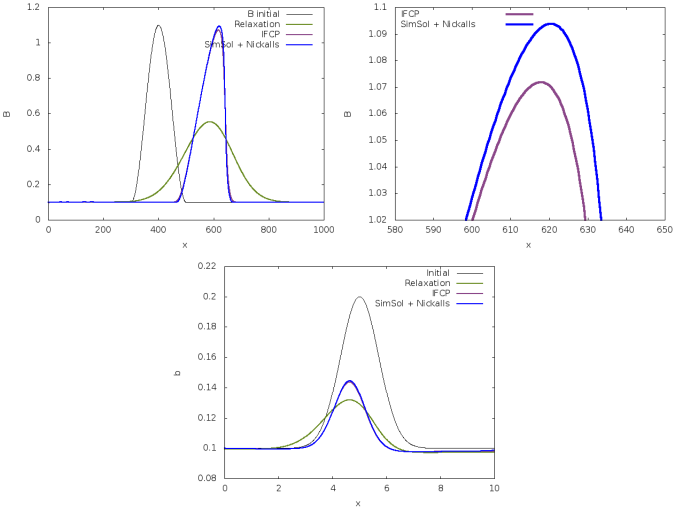

Figure: Bump in fluvial (top) and transcritical (bottom) flow.

Numerical results

Evolution of a bump in a torrential regime

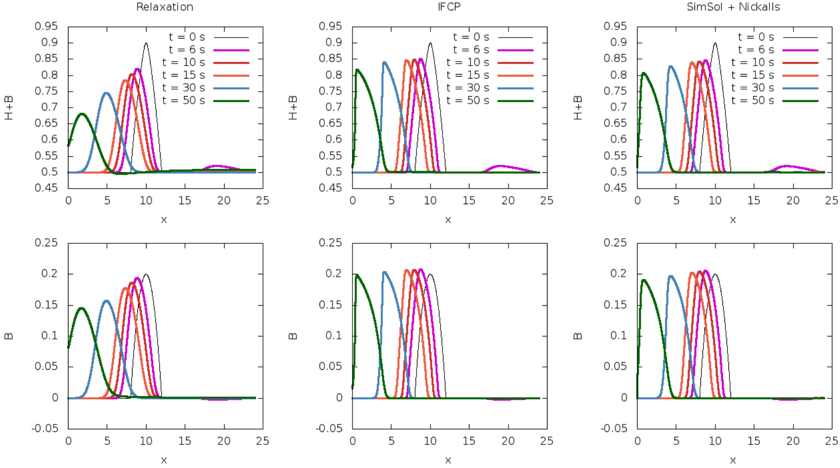

Figure: Antidune.

Numerical results
Dam break over a wet bed

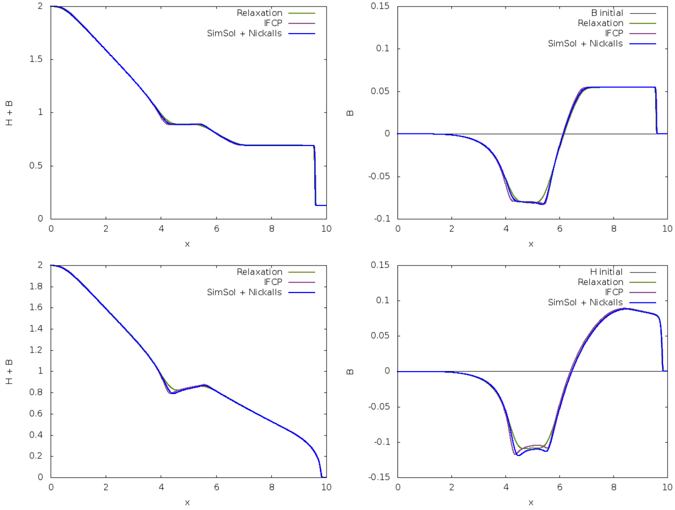

Figure: Dam break over wet (top) and dry (bottom) topographies.

Discussion

Discussion

Splitting vs non-splitting methods

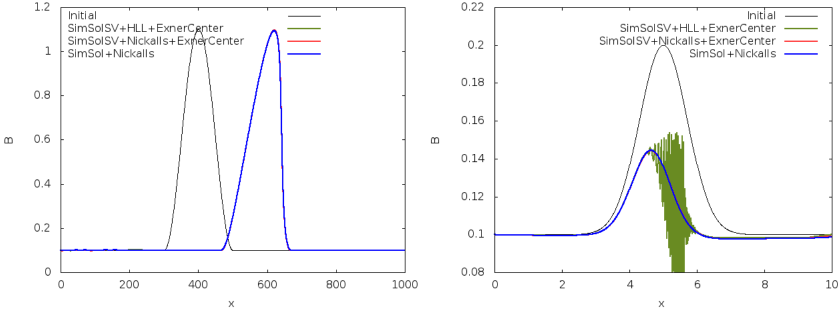

Figure: Bump on fluvial (left) and transcritical (right) regimes.

Discussion

Splitting vs non-splitting methods

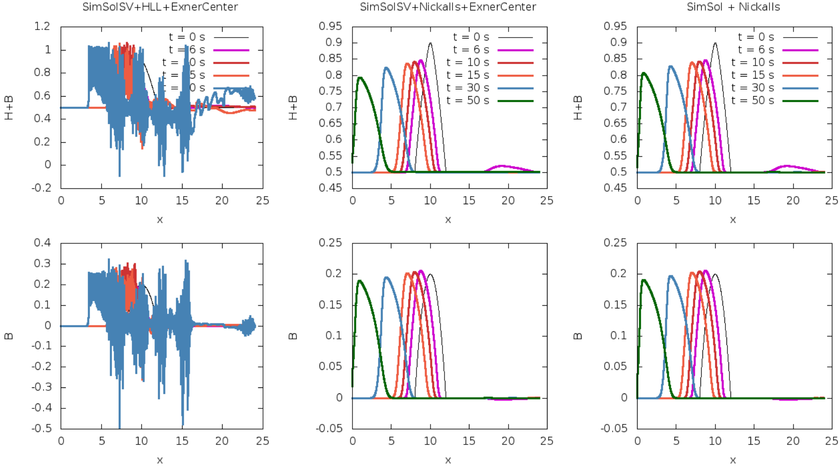

Figure: Antidune.

Discussion

Splitting vs non-splitting methods

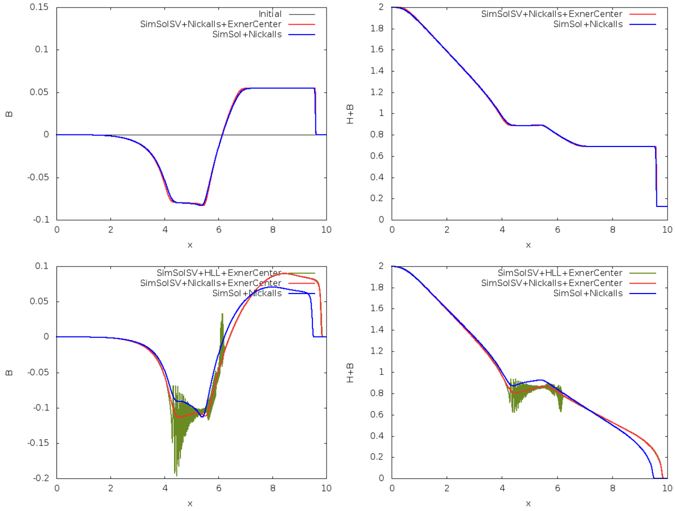

Figure: Dam break over wet (top) and dry (bottom) bed.

Thank you for your attention!